Spatio-temporal weighting for underwater source localization in the context of coherence loss

Riwal Lefort, Angélique Dremeau

SPATIO-TEMPORAL WEIGHTING FOR UNDERWATER SOURCE LOCALIZATION IN THE CONTEXT OF COHERENCE LOSS*

R Lefort ENSTA Bretagne, UMR-6285 Lab-STICC, Brest, France
A Drémeau ENSTA Bretagne, UMR-6285 Lab-STICC, Brest, France

* This work has been supported by the DGA/MRIS.

1 INTRODUCTION

In the field of underwater source localization, inversion remains the reference baseline. This approach consists of making a comparison between an analytical model of the expected acoustic pressure measured by an array antenna and the real captured one. By definition, the models are however limited to the knowledge available on the propagating medium while the propagated acoustic signal is subject to natural unpredictable ocean fluctuations. For instance, the internal waves may create spatio-temporal dynamics of the sound velocity, which introduces strong perturbations of the wave front[1]. The unpredictable acoustic wave echo due to a random seabed may produce such wave perturbations as well. The difficulty to integrate the random aspects of these natural phenomena into a physical model is the main source of the coherence loss observed in practice between sensors of a same antenna. In the literature, a lot of studies characterize a region in the ocean by analyzing the observed loss of coherence[2,3,6]. Some experiments have also been carried out in a tank to reproduce the loss of coherence on a measured signal, with the objective of proposing new processing methods[12,13].

In this paper, we are interested in the investigation of some processing methods that automatically correct the loss of coherence from the interpretation of the observed signal *in situ*. Among the various approaches we can think of, machine-learning techniques stand for an appropriate solution to deal with any losses of coherence[10] as they do not require any prior knowledge on the propagating medium but learn it instead. These techniques however require consistent training databases that may prevent their use in embedded acquisition systems. In this paper, we propose a new inversion method exploiting statistical knowledge on the acquired pressure field. If the perturbation is considered to be a stationary random process, the random characteristics are not depending on the time or, equivalently, the snapshot index. In that case, we can infer some parameters of the process, under an additional Gaussian assumption. Knowing the covariance matrix, it is consequently possible to cancel out any effects of the coherence loss[8,11]. But, the random ocean fluctuations make this random process not stationary in practice, leading to both spatial and temporal perturbation of the acoustic field. As a consequence, the coherence loss will not be the same from one snapshot, *e.g.* one time, to another. In a recent paper, this problem is addressed by a mixture model that classifies each snapshot according to two classes: “coherent” or “not coherent”[7]. This can be interpreted as a snapshot weighting method which gives a higher weight to those coherent snapshots. The problem may also be addressed from the point of view of sub-antenna processing[4]. In such a case, we suppose that each sub-antenna of each snapshot is locally coherent, thus, each sub-antenna independently applies a conventional localization method, such as a beamforming method.

In this paper, we propose a decision model that combines both the idea of sub-antenna processing and the concept of snapshot weighting. Unlike Cox’s works[4], our sub-antenna structure is not based on adjacent antenna pieces, each sub-antenna results from a sliding Gaussian function instead. In addition, unlike Ge’s works[7], we make the hypothesis that we know neither the signal power nor the noise power, and also, that we do not know the prior probability distribution of a coherent snapshot. Instead, we make use of the so-called “Mutual Coherence Function” to identify how coherent is a measured snapshot. In order to model the loss of coherence, we exploit a multiplicative noise, as recommended by Flatté[5]. This type of noise is indeed well-suited to model a perturbation attached

to an incoming wave, noticing that a multiplicative noise on the expected pressured field leads to an additive noise on the incoming wave phase. In the experiments, we show that our spatio-temporal weighting approach may outperform a conventional beam-former and some other baselines.

The paper is organized as follows. In section 2 we present the model used to characterize the coherent loss, in section 3 we present the model of source localization, in section 4 we propose experimental comparisons with baseline references, and we finally conclude in section 5.

2 MODEL OF LOSS OF COHERENCE

In this paper, we restrict our study to a single monochromatic source. Formally, let *f* be the emitting frequency of the source and θ its position. Note that this position may be the direction of arrival of plane waves or the {range, elevation} coordinates of spherical waves. Let $s_t(\theta) \in \mathbb{C}$ be the Fourier representation of the emitted signal at the frequency f at time t. Considering an array composed of K sensors, the model of a coherent received signal usually takes the following form:

$$\boldsymbol{y}_t = s_t(\theta)\boldsymbol{a}(\theta) + \boldsymbol{n}_t \tag{1}$$

Where $\boldsymbol{y}_t \in \mathbb{C}^{K\times 1}$ denotes a snapshot, *i.e.* a Fourier representation of the captured signal at frequency f at time t, and $\boldsymbol{a}(\theta) \in \mathbb{C}^{K\times 1}$ denotes a physical model of $\boldsymbol{y}_t$. For instance, when the source is far enough, we consider that the acoustic propagation can take the form of a plane wave:

$$\boldsymbol{a}(\theta) = \left[e^{j\frac{2\pi f\Delta\sin(\theta)}{c}}, e^{j\frac{2\pi f2\Delta\sin(\theta)}{c}}, \dots, e^{j\frac{2\pi fK\Delta\sin(\theta)}{c}}\right]^T \tag{2}$$

Where $.^T$ stands for the transpose operator, c denotes the sound celerity and Δ the distance between two consecutive sensors. The white additive noise $\boldsymbol{n}_t \in \mathbb{C}^{K\times 1}$ represents some electrical noise that follows a multivariate complex normal distribution: $p(\boldsymbol{n}_t) = \mathcal{CN}(\boldsymbol{0}, \sigma_t^2\boldsymbol{I}_K)$, with zero mean and a diagonal covariance matrix $\sigma_t^2\boldsymbol{I}_K$, with $\sigma_t \in \mathbb{R}$ proportional to the noise power and $\boldsymbol{I}_K \in \mathbb{R}^{K\times K}$ the identity matrix. In this paper, we assume that we do not know σ_t.

Let $\boldsymbol{\varphi}_t \in \mathbb{C}^{K\times 1}$ be a random vector modeling the loss of coherence due to the fluctuations of the propagating medium. We assume that it is distributed according to a zero-mean multivariate complex normal distribution of covariance matrix $\boldsymbol{\Sigma}_t \in \mathbb{R}^{K\times K}$: $p(\boldsymbol{\varphi}_t) = \mathcal{CN}(\boldsymbol{0}, \boldsymbol{\Sigma}_t)$. In comparison to the white noise $\boldsymbol{n}_t$ that has independent components, the components of $\boldsymbol{\varphi}_t$ are assumed to be statistically dependent. Formally, it is implemented into the observation model (1) as a multiplicative noise:

$$\boldsymbol{y}_t = s_t(\theta)[\boldsymbol{a}(\theta) \times \boldsymbol{\varphi}_t] + \boldsymbol{n}_t \tag{3}$$

Where the operator $\times$ denotes an element-by-element vector multiplication.

Let us now consider some more interpretations. The model of multiplicative noise is not new in the literature. Flatté has considered this model to study and statistically characterize different regimes of fluctuations[5]. De facto, multiplicative complex noise is well-suited to model additive phase noise (*and* some kind of attenuation) on incoming waves. Here, we assume a not-diagonal covariance matrix $\boldsymbol{\Sigma}_t$, such that we are able to statistically model the sensor dependencies. In practice, it is possible to relate the elements of $\boldsymbol{\Sigma}_t$ to the local coherence length of the fluctuation, say L_c, so that it validates the effectively observed correlation between two sensors of the array, depending on their distance. Hence each element $\boldsymbol{\Sigma}_t(k_1, k_2)$ of the covariance matrix is Gaussian-like expressed as:

$$\boldsymbol{\Sigma}_t(k_1, k_2) = e^{\frac{-0.5(k_1-k_2)^2}{{L_c}^2}} \tag{4}$$

The way the signal is coherent in time and space is then directly modeled by the way the sensors are correlated. In figure 1, we show three realizations of three different random processes that we have simulated. In this figure, we plot the phase of the coherence loss $\arg(\boldsymbol{\varphi}_t)$ for each sensor of each snapshot. For instance, in figure 1-a, by changing the covariance matrix $\boldsymbol{\Sigma}_t$ at each snapshot, we have been able to generate a loss of coherence that is not stationary, the coherence loss being spatially constant. In figure 1-b, we have simulated a loss of coherence from a single covariance matrix $\boldsymbol{\Sigma}_t$, making the realization stationary, but the loss of coherence is not spatially constant in the

array: the first part of the antenna is more coherent than the second part. In figure 1-c, we combine the two previous cases: the random process that generate $\boldsymbol{\varphi}_t$ is not stationary and the loss of coherence is not spatially constant. This paper takes place in the context of the general scenario of figure 1-c that involves losses of coherence that are not constant in both space and time.

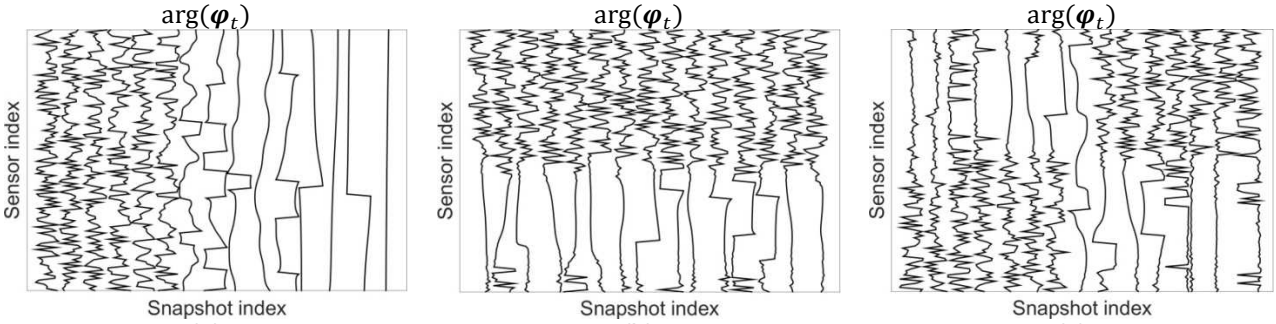

Figure 1. We plot the phase of the loss of coherence $\arg(\boldsymbol{\varphi}_t)$ as a function of both the sensor index and the snapshot index. Figure 1-a: the random process $\boldsymbol{\varphi}_t$ is depending on time and the loss of coherence is spatially constant. Figure 1-b: the random process $\boldsymbol{\varphi}_t$ is not depending on time and the loss of coherence is not spatially constant. Figure 1-c: the random process $\boldsymbol{\varphi}_t$ is not depending on time and the loss of coherence is not spatially constant.

3 MODELS OF SOURCE LOCALIZATION

3.1 Conventional beamforming

The conventional beamforming is used for any source signal which is modelled from the expression (1). It consists in finding the source position that maximizes the estimated source signal intensity:

$$\hat{\theta} = \arg\max_{\theta} \sum_{t=1}^{T} |\hat{s}_t(\theta)|^2 \tag{5}$$

Where T denotes the number of snapshots. The optimization problem (5) is greedy solved by grid search. The estimated source signal intensity is the solution of the square error minimization problem:

$$\hat{s}_t(\theta) = \arg\min_{s_t(\theta)} \|\boldsymbol{y}_t - s_t(\theta)\boldsymbol{a}(\theta)\|^2 \tag{6}$$

The solution of (6) being given by $\hat{s}_t(\theta)=\boldsymbol{a}(\theta)^{\mathrm{H}}\boldsymbol{y}_t/\boldsymbol{a}(\theta)^H\boldsymbol{a}(\theta)$, the conventional beam-former thus takes the form of:

$$\hat{\theta} = \arg\max_{\theta} \sum_{t=1}^{T} \left| \frac{\boldsymbol{a}(\theta)^{\mathrm{H}}\boldsymbol{y}_t}{\boldsymbol{a}(\theta)^H\boldsymbol{a}(\theta)} \right|^2 \tag{7}$$

3.2 Temporal weighting

In this part, we consider that the source signal is subject to some loss of coherence accordingly to expression (3). In addition, we consider that the loss of coherence $\boldsymbol{\varphi}_t$ is random sampled from a random process that is not stationary but spatially constant. Examples of such realizations are given in figure 1-a. Ge has proposed a method to weight each snapshot contribution[7], but it requires to know some environmental parameters such as the signal power, the white noise power, and also, the prior probability that a snapshot is coherent. Instead, in this paper, the method we investigate is not depending of such crucial parameters. We just extend the expression (5), by adding a weighting variable α_t that indicates how coherent a snapshot is:

$$\hat{\theta} = \arg\max_{\theta} \sum_{t=1}^{T} \alpha_t \left| \frac{\boldsymbol{a}(\theta)^{\mathrm{H}} \boldsymbol{y}_t}{\boldsymbol{a}(\theta)^{H} \boldsymbol{a}(\theta)} \right|^2 \quad (8)$$

The weighting parameter is expressed as follows:

$$\alpha_t = \int |g_k(\boldsymbol{y}_t)| \, dk \quad (9)$$

Where $g_k(\boldsymbol{y}_t)$, also called the "Mutual Coherence Function"[3,12,13], measures the averaged statistical correlation in the complex domain between two sensors separated by k sensors:

$$g_k(\boldsymbol{y}_t) = \frac{\sum_n \boldsymbol{y}_t(n)^H \boldsymbol{y}_t(n+k)}{\sqrt{\sum_n |\boldsymbol{y}_t(n)|^2} \sqrt{\sum_n |\boldsymbol{y}_t(n+k)|^2}} \quad (10)$$

For a given measured snapshot, if all the sensors are coherent, thus $|g_k(\boldsymbol{y}_t)| = 1$ for all k and thus $\alpha_t = 1$. On the contrary, in the presence of coherence loss, we observe that $|g_k(\boldsymbol{y}_t)|$ tends toward 0 when k is increasing, by consequence α_t tends toward 0.

3.3 Spatial weighting

In this section, we design a sub-antenna model from a weighting vector $w_k \in \mathbb{R}^{K \times 1}$, where:

$$w_k = \left[e^{-0.5\left(\frac{k-1}{\gamma}\right)^2}, \quad \ldots, e^{-0.5\left(\frac{k-K}{\gamma}\right)^2} \right]^T \quad (11)$$

The shape of each sub-antenna is therefore drawn from a Gaussian-like function, the parameter γ being setting the sub-antenna length. Doing so, we aim to mimicking the front distortion of the incoming waves induced by some fluctuations modeled as in (3), the parameter γ playing a similar role as the coherence length $L_{c.}$. We ensure that each sensor is a centroid of coherence by making the Gaussian sliding along the antenna. There are consequently as many sub-antennas as there are sensors in the antenna. The beam-former therefore takes into account the contribution of each snapshot of each sub-antenna:

$$\hat{\theta} = \arg\max_{\theta} \sum_{k=1}^{K} \sum_{t=1}^{T} \left| \hat{s}_{k,t}(\theta) \right|^2 \quad (12)$$

Where $\hat{s}_{k,t}(\theta) \in \mathbb{C}$ denotes the Fourier representation of this signal in θ from the point of view of the sub antenna. In addition, we make the major assumption that the sensors are locally coherent. In other words, we consider that there is not any loss of coherence in a sub antenna drawn by w_k. Accordingly, the model (3) can be rewritten in its coherent form:

$$[\boldsymbol{w}_k \times \boldsymbol{y}_t] = s_{k,t}(\theta) \boldsymbol{a}(\theta) + \boldsymbol{n}_t \quad (13)$$

The estimated source signal intensity is the solution of the square error minimization problem:

$$\hat{s}_{kt}(\theta) = \arg\min_{s_t(\theta)} \left\| [\boldsymbol{w}_k \times \boldsymbol{y}_t] - s_{k,t}(\theta) \boldsymbol{a}(\theta) \right\|^2 \quad (14)$$

This leads to the following sub-antenna beam-former:

$$\hat{\theta} = \arg\min_{\theta} \sum_{k=1}^{K} \sum_{t=1}^{T} \left| \frac{\boldsymbol{a}(\theta)^{\mathrm{H}} [\boldsymbol{w}_k \times \boldsymbol{y}_t]}{\boldsymbol{a}(\theta)^{H} \boldsymbol{a}(\theta)} \right|^2 \quad (15)$$

3.4 Spatio-temporal weighting

The method we investigate in this section combines both the spatial weighting of section 3.3 and the temporal weighting of section 3.2. The proposed beam-former is a combination of equations (8) and (15):

$$\hat{\theta} = \arg\max_{\theta} \sum_{k=1}^{K} \sum_{t=1}^{T} \alpha_{k,t} \left| \frac{\boldsymbol{a}(\theta)^{\mathrm{H}} [\boldsymbol{w}_k \times \boldsymbol{y}_t]}{\boldsymbol{a}(\theta)^{H} \boldsymbol{a}(\theta)} \right|^2 \quad (16)$$

According to section 3.2, the weight $\alpha_{k,t}$ is a coherence indicator of the tth snapshot received by the kth sub-antenna, drawn by the $w_k$weighting:

$$\alpha_{k,t} = \int \left| g_k(\boldsymbol{y}_{k,t}) \right| dk \quad (17)$$

Where $g_k(\boldsymbol{y}_{k,t})$ is defined as in equation (10). This approach allows us to weight each sub-antenna according to its observed intrinsic loss of coherence.

In figure 2-b, we give the evaluated $\{\alpha_{k,t}\}$, for all k, t, for the particular realization of the sampled noise $\boldsymbol{\varphi}_t$ given in figure 2-a. In this experiment, we have random sampled a snapshot before we have added the coherent noise $\{\boldsymbol{\varphi}_t\}$ and computed $\{\alpha_{k,t}\}$ by using equation (17). The signal-to-noise ratio related to the additive white noise $\boldsymbol{n}_t$ is infinite (noiseless case). As expected, the more the coherence loss $\boldsymbol{\varphi}_t$, the closer to 0 the weighting parameter $\alpha_{k,t}$. On the contrary, when the loss of coherence is constant between some sensors, the corresponding weighting parameter is close to 0.

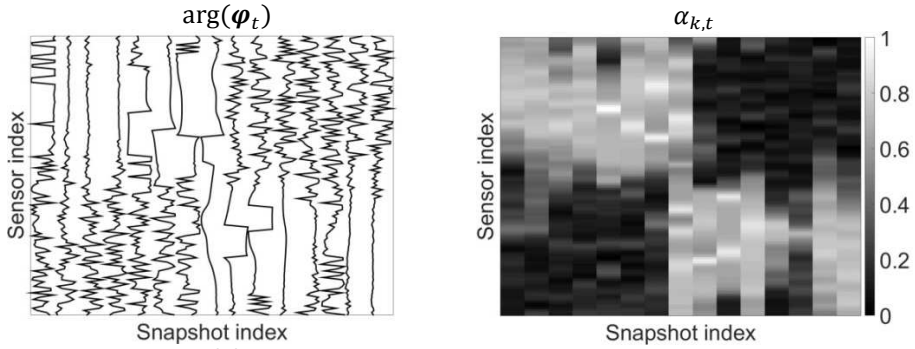

(a) (b)

Figure 2. In figure 2-a, we show $\arg(\boldsymbol{\varphi}_t)$ the phase of a dynamic random loss of coherence as a function of both the snapshot index and the sensor index. In figure 2-b, we show the corresponding weighting parameter $\alpha_{k,t}$.

4 EXPERIMENTS

4.1 Simulation protocol

We consider the problem of assessing the direction of arrival (DOA) of a plane wave. The distance Δ between two consecutive sensors is chosen such that the Shannon property remains valid: $\Delta = \frac{c}{2f}$. In this context, the replica $\boldsymbol{a}(\theta)$ is given by model (2). We consider an antenna composed of $K = 32$ sensors. The inverse problem is solved by searching in a grid 128 possible DOA in $\left[\frac{-\pi}{3}, \frac{\pi}{3}\right]$. We consider $I = 5000$ Monte Carlo iterations to compute an average localization error. More precisely, at each iteration $i \in \{0, \ldots, I\}$, we random sample a DOA $\theta_i \in \left[\frac{-\pi}{3}, \frac{\pi}{3}\right]$. Let $\hat{\theta}_i$ be the estimated DOA, we then compute the normalized localization error and we deduce the mean localization error from: $\frac{3}{2\pi I}\sum_{i=1}^{I}\left|\theta_i - \hat{\theta}_i\right|$.

We generate the received pressure field according to model (3). We consider the following scenario where the first snapshot is assumed to be the only one "partly coherent". This is illustrated in figure 3-a and b by the covariance matrices used to draw the coherence losses of the snapshots. More precisely, the loss $\boldsymbol{\varphi}_1$ of the first snapshot is generated from the covariance matrix $\boldsymbol{\Sigma}_1$ that is shown in figure 3-a. This covariance matrix is such that the coherence loss is weak (the coherence length equals $L_c = 10$ sensors) on the first part of the antenna, while it is strong on the other part of the antenna, with a coherence length of $L_c = 0.1$ sensors. For the other snapshots, the loss of coherence is assumed also strong, with a coherence length of $L_c = 0.1$ sensors along the antenna. The covariance matrix $\boldsymbol{\Sigma}_t$, for all $t \neq 1$, is shown in figure 3-b. Note that, in order to random sample $\boldsymbol{\varphi}_t$, we must ensure that the covariance matrix $\boldsymbol{\Sigma}_t$ is positive definite. We therefore replace $\boldsymbol{\Sigma}_t$ by a nearest positive one: $\boldsymbol{\Sigma}_t \leftarrow \left(\boldsymbol{\Sigma}_t{}^{\mathrm{H}}\boldsymbol{\Sigma}_t\right)^{1/2} + K\boldsymbol{I}_K$.

In this paper, the free parameter γ in (11) is empirically set to $\gamma = 4$ sensors, whatever the coherence length L_c. In this regard, it is worth noticing that the link between both parameters L_c and γ is not obvious. The first one is part of a probabilistic model, and as such, will be representative of an *average* behavior of the coherence loss, while the other set deterministically the weights given to each sensor within the sub-antennas. In practice, this choice of $\gamma = 4$, although clearly not optimal, was sufficient to get the good results presented in the next subsection. We discuss further possible optimization developments of parameter γ in section 4.3.

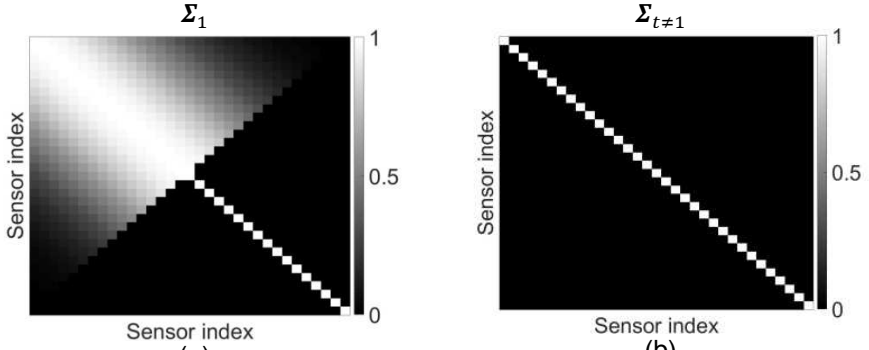

Figure 3. The loss of coherence $\boldsymbol{\varphi}_1$ associated to the first snapshot is random sampled from the covariance $\boldsymbol{\Sigma}_1$ shown in figure 3-a. All the next snapshots are generated by using a random loss of coherence which is sampled from the covariance matrix $\boldsymbol{\Sigma}_{t\neq 1}$ shown in figure 3-b.

4.2 Results

Figure 4 compares the four localization methods presented in section 3. Each subfigure reports the average localization error as a function of a particular parameter. In figures 4-a-c-d, the experimental setup is such that the proportion of coherent sensors in the first snapshots is set to 0.5 according to the covariance matrix in figure 3-a. In figures 4-b-c-d, the signal-to-noise ratio (SNR) of the random white noise $\boldsymbol{n}_t$ is set to 20dB. In figures 4-a-b-d, there are $T = 10$ snapshots.

In figure 4-a, the average localization error is reported as a function of the SNR of the random white noise $\boldsymbol{n}_t$. As expected, the less the SNR the more the localization error, but in a favorable case of positive SNR, we find that the spatio-temporal weighting outperforms the other approaches by a factor of two. We also notice the improvement brought by a spatial weighting and a temporal weighting that both outperform a conventional beam-forming.

In figure 4-b, the localization error is reported as a function of the proportion of coherent sensors in the first snapshot. When the proportion is set to 0, none of the sensors are coherent in the first snapshot, making the localization task very tough and the error very high. On the contrary, we observe a very low localization error when this proportion tends toward one, all the sensors being consequently coherent. In between, when the proportion between the number of coherent and not coherent sensors is more balanced, the spatio-temporal approach is able to identify the informative part which makes the localization error decreased.

In figure 4-c, the localization error is reported as a function of the number of snapshots. We note that the spatio-temporal processing drastically outperforms any other approach even if the localization error increases when the number of snapshots increases. The reason why the error increases as the number of snapshots increases is that all the snapshots we add are fully not coherent, as describes in section 4.1.

In figure 4-d, the localization error is reported as a function of the coherence length L_c (equation (4)) in the coherent part of the first snapshot. Similarly to the previous results, we note that the proposed spatio-temporal outperforms by a factor of two.

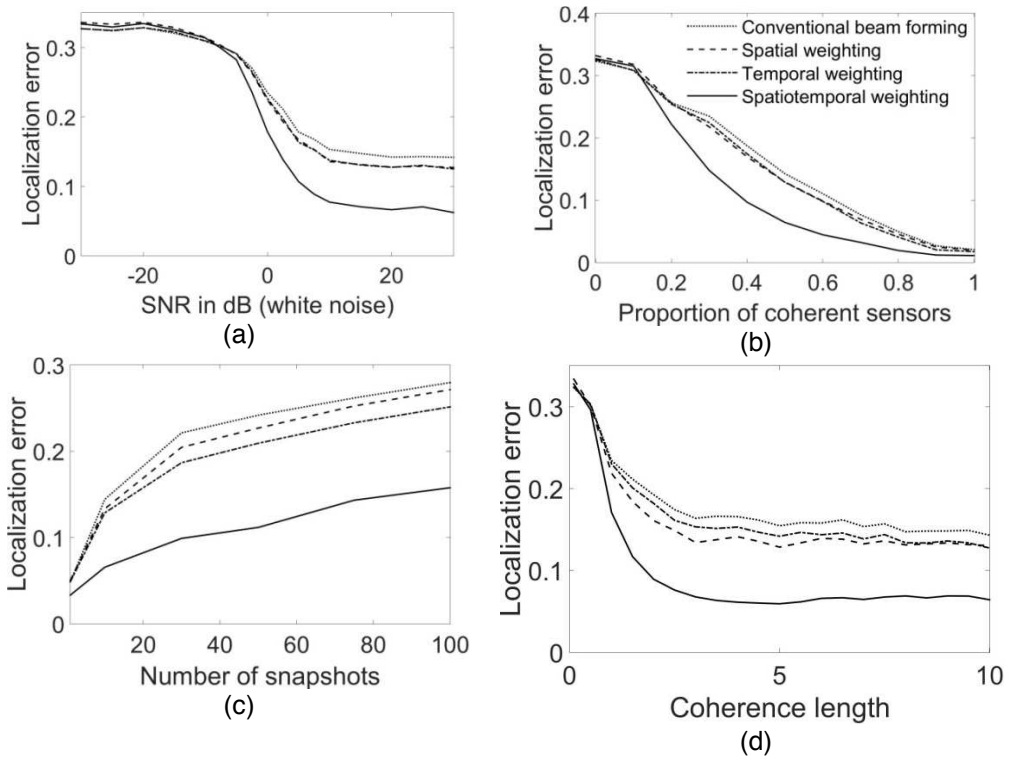

Figure 4. We compare the localization performance of the methods presented in section 3. In figure, 4-a, the average localization error is reported as a function of the Signal to Noise Ratio (SNR) of the white noise $\boldsymbol{n}_t$. In figure 4-b, it is reported as a function of the proportion of coherent sensors in the first snapshot. In figure 4-c, it is reported as a function of the number of snapshots. In figure 4-d, it is reported as a function of the coherence length L_c in equation (4).

4.3 Discussion and perspectives

On the first hand, the simulation results we have obtained are very encouraging and promising. Figure 4 indeed shows that our proposed method outperforms some well-known baselines in the scenario that we have considered. On the second hand, it raises numerous questions about both the applicability and the perspective of the approach.

The methods, called “spatial weighting” and “spatio-temporal weighting”, respectively presented in sections 3.3 and 3.4, are roughly based on sub-antenna processing. The consequence of such a smaller antenna is a reduction of the spatial resolution. This may be an issue in multi-source cases. Especially, the averaging effect may, if not increase, at least fail to improve the localization error in the case of low SNR. As an example, in figure 4-a, in the case of low SNR, there is no improvement by using these sub-antenna approaches. We therefore encourage the development of high-resolute versions of sub-antenna processing. For instance, a techniques exploiting more prior information on the sources, as sparsity, may be adapted in that specific case[9].

In this paper, the free parameter γ has been set empirically. Instead, this could be addressed from the point of view of an optimization problem that consists of finding the best parameter value, the one that matches the best with the data. For instance, a dynamic parameter $\gamma_{k,t}$ that depends on both the sensor index and on the snapshot index would be interesting. In the example of figure 1-b, a low value should be reached in the noisy part of the antenna, while a high value should be reached in the coherent part. Moreover, it should be possible to define the vector w_k as a discrete vector, the objective being to directly optimize its components. For instance, the objective function to optimize could be dependent on the Mutual Coherence Function integration (17).

Finally, it would be of interest to evaluate the proposed approach on a real dataset acquired *in situ*. The data measurements carried out by Badiey *et. al*. reveal a huge temperature dynamics and, consequently, a spatio-temporal variation of the sound velocity profile[1]. The effects of such observed losses of coherence could be dealt with our proposed approach. To complete this task, it is possible to extend the model (2) to broadband signal as well as to multi modal propagated signals in shallow water.

5 CONCLUSION

We have proposed a method to deal with the problem of spatio-temporal dynamic fluctuation of a propagation channel. This method combines the optimality of the sub-antenna processing as well as the idea of weighting the snapshots according to their degree of coherence.

The approach is assessed through various synthetic experimentations paving the way of promising developments. Future work will in particular focus on introducing more prior information on each sub-antenna processing in order to deal with the multi-source case.

6 REFERENCES

1. M. Badiey and L. Wan, Statistics of nonlinear internal waves during the shallow water 2006 experiment, Journal of Atmospheric and Oceanic Technology, Vol 33, 2016.
2. W.M. Carey, The determination of signal coherence length based on signal coherence and gain measurements in deep and shallow water, Journal of the Acoustic Society of America, Vol 104(2), 1998.
3. J.M. Collis, T.F. Duda, J.F. Lynch and H.A. DeFerrari, Observed limiting cases of horizontal field coherence and array performance in a time-varying internal wavefield, Journal of the Acoustic Society of America, Vol 124(3), 2008.
4. H. Cox, Line array performance when the signal coherence is spatially dependent, Journal of the Acoustic Society of America, Vol 54, 1973.
5. R. Dashen, W.H. Munk, K.M. Watson and F. Cachariasen, Sound Transmission through a Fluctuating Ocean, 1st ed, S.M. Flatté, Ed. Cambridge University Press, June 1979.
6. T.F. Duda, J.M. Collis, Y.-T. Lin, A.E. Newhall, J.F. Lynch, H.A. DeFerrari, Horizontal coherence of low-frequency fixed-path sound in a continental shelf region with internal wave activity, Journal of the Acoustic Society of America, Vol 131(2), 2012.
7. H. Ge and I.P. Kirsteins, Lucky ranging with towed arrays in underwater environments subject to non-stationary spatial coherence loss, Proceedings of the International Conference on Acoustics, Speech, and Signal Processing, 2016.
8. A. B. Gershman, C.F. Mecklenbraüker, J.F. Böhme, Matrix fitting approach to direction of arrival estimation with imperfect spatial coherence of wavefront, IEEE Transaction on Signal Processing, Vol 45(7), 1997.
9. P. Gerstoft, A. Xenaki, C.F. Mecklenbräuker, Multiple and single snapshot compressive beamforming", Journal of the Acoustic Society of America, Vol 138(4), 2015.
10. R. Lefort, G. Real, A. Drémeau, Direct regressions for underwater acoustic source localization in fluctuating oceans, Applied Acoustics, Vol 116, 2016.
11. A. Paulraj and T. Kailath, Direction of arrival estimation by eigen structure methods with imperfect spatial coherence of wave fronts, Journal of the Acoustic Society of America, Vol 83(3), 1988.
12. G. Real, X. Cristol, D. Habault, D. Fattaccioli, Influence of de-coherence effects on sonar array gain: scales experiment, simulations and simplified theory comparison, Underwater Acoustics Conference & Exhibition, 2015.
13. G. Real, X. Cristol, D. Habault, D. Fattaccioli, RAFAL: Radom Faced Acoustic Lens used to model internal waves effects on underwater acoustic propagation, Underwater Acoustics Conference & Exhibition, 2015.